

ABSTRACT

Title of Document: A SPIKE-BASED HEAD-MOVEMENT AND ECHOLOCATION MODEL OF THE BAT SUPERIOR COLLICULUS.

Matthew Robert Runchey, Master of Science,
2013

Directed By: Associate Professor Timothy Horiuchi
Department of Electrical Engineering and
Institute for Systems Research

Echolocating bats use sonar to sense their environment and hunt for food in darkness. To understand this unusual sensory system from a computational perspective with aspirations towards developing high performance electronic implementations, we study the bat brain. The midbrain superior colliculus (SC) has been shown (in many species) to support multisensory integration and orientation behaviors, namely eye saccades and head turns. Previous computational models of the SC have emphasized the behavior typical to monkeys, barn owls, and cats. Using unique neurobiological data for the bat and incorporating knowledge from other species, a computational spiking model has been developed to produce both head-movement and sonar vocalization. The model accomplishes this with simple neuron equations and synapses, which is promising for implementation on a VLSI chip. This model can serve as a foundation for further developments, using new data from bat experiments, and be easily connected to spiking motor and vocalization systems.

A SPIKE-BASED HEAD-MOVEMENT AND ECHOLOCATION MODEL OF
THE BAT SUPERIOR COLLICULUS

By

Matthew Robert Runchey

Thesis submitted to the Faculty of the Graduate School of the
University of Maryland, College Park, in partial fulfillment
of the requirements for the degree of
Master of Science
2013

Advisory Committee:

Professor Timothy Horiuchi, Chair

Professor Pamela Abshire

Professor Jonathan Simon

© Copyright by
Matthew Robert Runchey
2013

Acknowledgements

I would like to thank Dr. Timothy Horiuchi for his continual support throughout this research. Without his immense amount of guidance, knowledge, and patience, my understanding of the subject would not compare.

Table of Contents

Acknowledgements.....	ii
Table of Contents.....	iii
List of Figures.....	v
Chapter 1: Introduction.....	1
1.1 The Mammalian Superior Colliculus Structure.....	1
1.2 The Bat Superior Colliculus.....	2
1.3 Superior Colliculus Tuning in the Echolocating Bat.....	4
1.4 Non-Mammalian Superior Colliculus Specializations.....	5
Chapter 2: Biological Data from the Bat Superior Colliculus.....	6
2.1 Spatially Selective Auditory Responses.....	6
2.2 Head-Movement and Vocalization by Microstimulation.....	8
2.3 Vocal Premotor Activity.....	10
Chapter 3: Existing Computational Models of the Superior Colliculus.....	13
3.1 Trappenberg et al. (2001).....	13
3.2 Arai and Keller (2005).....	15
3.3 Current Non-Spiking Model.....	16
Chapter 4: A Spike-Based Model of the Bat Superior Colliculus.....	22
4.1 Neuron Model Equations.....	23
4.2 Connecting the Components.....	30
4.3 VLSI Considerations.....	32
Chapter 5: Future Work.....	33

Appendix.....	34
Bibliography	41

List of Figures

Figure 1. Bat brain structures relevant to the superior colliculus [1]

Figure 2. Delay profiles for 3D colliculus neurons [5].

Figure 3. Microstimulation response profiles of neurons [18]

Figure 4. Sonar call duration vs. pulse interval [19].

Figure 5. 1D Monkey Superior Colliculus model [25].

Figure 6. System model for SC that generates saccades [27]

Figure 7. 2D bat superior colliculus model block diagram.

Figure 8. SNr and SC spiking 2D model responses.

Figure 9. Buildup and burst neuron responses over time

Figure 10. Motor neuron responses to SC burst activity.

Figure 11. Spiking model of the SC

Figure 12. Layout of SNr and SC layers.

Figure 13. Neural integrator structure

Figure 14. Neural integrator three unit example

Figure 15. Larger neural integrator spike raster

Figure 16. Spiking SNr and SC model 2D stimulation response

Chapter 1: Introduction

1.1 The Mammalian Superior Colliculus Structure

The superior colliculus (SC), sometimes referred to as the optic tectum in non-mammalian species - and heavily studied in the visual domain - is a layered, bilobed brain structure. The superficial and intermediate layers receive raw and processed sensory input from the visual, auditory, and other sensory systems, while the deep layers project to the brainstem, which have nuclei that connect to motor systems such as the eye and neck muscles. Some of the intermediate layers have more complex afferents and efferents, both sensory and motor. Since several information pathways in the brain converge on the SC, it is thought that they are integrated here into a common sensorimotor representation and translated into actionable responses, such as saccades (quick eye movements) and head and/or pinnae movements. The SC informs behavioral responses in head-centered space. The layers organize topographically, such that a locus or ‘bump’ of activity will elicit a response toward the corresponding point in space.

In species where eye movements are the dominant form of sensor orientation, the responses have largely been described from the point of view of the visual system. Visually, the map is laid out in retinotopic coordinates and the evoked responses are

saccades and head turns. Some non-mammalian species have relatively larger tecta, such as fish and birds.

The SC is an evolutionarily old brain structure of the vertebrate midbrain, with distinguishing characteristics in different species. While some aspects of the SC remain more consistent – such as the fact that it contains dense optic tract afferents and strong inputs to deeper layers – others vary more, such as the total number of layers or the types of cells each layer contains. In vertebrates with a less developed cerebral cortex, the tectum may account for a significant portion of the overall brain matter.

1.2 The Bat Superior Colliculus

While microchiropteran bats are not blind, their vision is relatively low resolution and dominated by slowly responding rod photoreceptors. They rely heavily on echolocation (as opposed to vision) for navigation and hunting. They detect the location of objects in their environment by emitting primarily-ultrasonic frequency chirps and listening for echoes. The retinal projection to the SC in echolocating bats occupies only a very small zone in the surface layers, and the intermediate layers mostly contain large auditory afferents [1]. Efferents to ear, head, and body orientation muscles originate in the deep layers, instead of the more superficial eye-saccade related areas. In addition, echo timing influences which neurons in each

layer activate, and it is thought that the timing of these neuron activations directly influences future sonar chirps [2]. These correlations suggest that the SC has the same role for auditory behavior in bats as for visual-guided actions in other vertebrates. Figure 1 shows the key areas of the SC that are thought to play a role in converting sensory information into signals sent to premotor and motor structures controlling head-movements and echolocation calls [1].

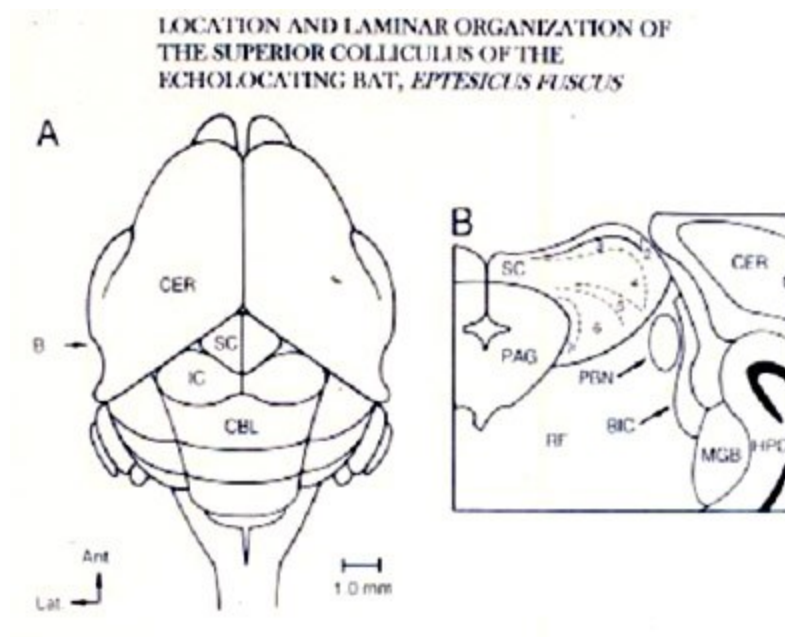


Figure 1 (A. Shows the dorsal view of the brain of a species of bat, *Eptesicus Fuscus*. B. A cross-section showing laminar structures of the SC. Abbreviations: PAG = Periaqueductal Grey, MGB = Medial Geniculate Body, IC = Inferior Colliculus, CLB = Cerebellum [1].

1.3 Superior Colliculus Tuning in the Echolocating Bat

As a bat flies and forages for food in darkness, it emits ultrasonic vocal signals and listens for the echoes [2]. Differences in arrival time, intensity, and spectrum between the ears allow the bat to localize objects and prey, and the time delay determines distance [3, 4]. Using extracellular recording techniques, it was shown that spatially selective neurons in the superior colliculus of the bat were tuned to a target range [5]. In a separate study, over half of the measured neurons in the SC were found tuned to have narrow, intermediate, or broad tuning curves, and most 3D neurons had response latencies less than 12.5 ms, though the full range of latencies was 3.6 to 20 ms [6]. The neurons were also tuned to specific frequencies, and minimum thresholds were found to hold within one frequency octave upward and downward sweeping FM sonar stimuli (frequencies further than an octave away didn't evoke a response). They further state that these findings suggest that there is a spatial map within the SC, and that its role is primarily in the head's orientation to a sound source.

This tuning is not unique to the bat. Auditory space gets encoded in the SC in ferrets, with some neurons tuned to single regions in space [7]. Other neurons were either hemifield or bilobed response profiles. It was also suggested that the brachium of the inferior colliculus sends signals to the SC that are already somewhat selective for the sound's azimuth and elevation, which are sharpened in the SC layers.

What results is a two-dimensional map of auditory space across the horizontal extent of the midbrain nucleus, including the substantia nigra reticula (or SNr) [8, 9,

10]. The arrangement of the neurons and layers provides a computationally and spatially efficient path for integrating multi-sensory cues and allows head orientation using a common premotor pathway [11, 12].

1.4 Non-Mammalian Superior Colliculus Specializations

In barn owls, the optic tectum contributes largely to the metric and kinetic properties of saccadic head movements [13], producing analogous results as previous studies on saccadic eye movements in primates and head movements in the cat. Cats have a very limited eye movement range, so head-movements are more prevalent than in a primate. This collicular activity produces a much different result than in a monkey, which has much more freedom of eye motion. Masino and Knudsen also demonstrate similar phenomena in the barn owl, stating that there is an abstract code underlying movements of the head of the barn owl coded to the retinotopic space (neural visual map) in the optic tectum before the motor neuron code for muscle tensions, suggesting that the SC provides an intermediate step in the transformation of sensation into motor behavior [14].

In amphibians, the optic tectum was shown to play a role in crucial prey-catching and predator avoidance tasks, but was unable to directly account for the stimulus responses (e.g. premotor outputs) [15]. In the rattlesnake optic tectum, bimodal neurons that receive sensory input from the retina and infrared-sensing neurons created activity in the superior colliculus and oriented toward biologically important objects [16].

Chapter 2: Biological Data from the Bat Superior Colliculus

The previously discussed comparative animal studies suggest that the SC has a role in shaping saccadic, smooth pursuit, and vergence head, pinnae, and body movements in various species, as well as other orienting, target, and evasion behaviors in others. Using this anatomical background, a few studies have focused on extracellular recordings to study the neural activity of an echolocating bat's superior colliculus. The findings of these studies are key components of the computational model presented in chapter 4.

2.1 Spatially Selective Auditory Responses

Valentine and Moss (1997) [5] used single-unit stimulations and implanted electrode measurements to test the spatial properties of SC cells from both extracellular recordings and free-field auditory stimulation. From the nearly 100 neurons measured, two groups of spatially tuned neurons appeared: first, a class that seemed tuned to two-dimensional coordinates, selective to azimuth and elevation but not echo timing (i.e., not object range) – and a second class that was three-dimensional, and was thus selective to echo timing, azimuth, and elevation. Two-thirds of the neurons were 2D and most of them fired maximally to a small hemifield 30 degrees laterally of the midline in the contralateral hemifield. They were also responsive to elevations within 18 degrees above and below.

Three dimensional neurons, with the additional dimension being time, determine the target range of echoes in the neural representation. In all of the 3D

units studied, they were maximally active when the vocalization and delayed echo pair were separated by a specific time period. Figure 2 below shows the results of best echo delay pairings and range sensitivity. The mean delay was 13.5 ms with a deviation of 8.1 ms, and 90% of the neurons were tuned between 4 and 20 msec. While most of the delays were tuned specifically to a time, some had broader responses or bimodal responses.

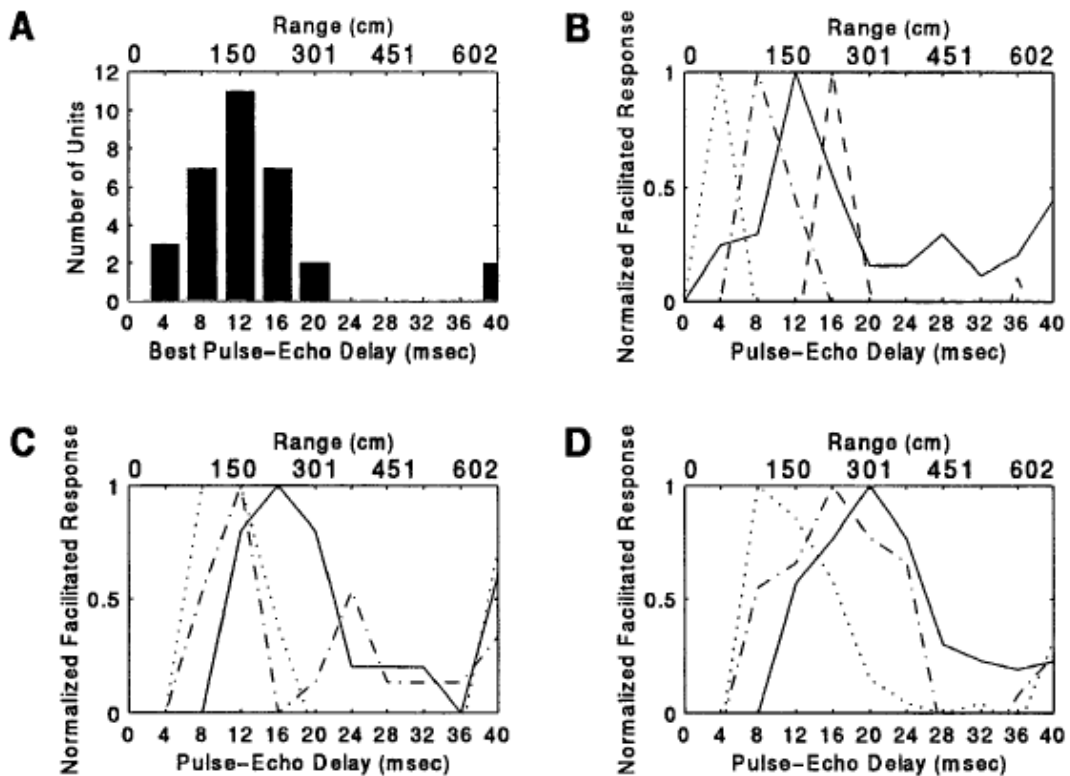


Figure 2. A) shows the overall best delays (BD) for the 3D neurons. They had varying response profiles, with B) being selective, C) being twin-peaked, and D) being broadly facilitated. Each line on those graphs are for individual neurons in the experiment [5].

The results of Valentine's and Moss's findings suggest that a 2D map of auditory space is not entirely topographic, but rather that most of the neurons are tuned to only azimuths in the 30-40 degree span from the center of view. As the directionality of a sonar call is quite narrow, this seems conventional, as echoes from ranges outside of the beam would not likely contain much energy from the sonar call or information. The delay-tuning mechanism suggested will also play a role in modeling, as the delay of these neurons could serve as a trigger as to when to start another vocalization, after the previous information has been received, processed, and the head turned. These 3D neurons help coordinate the timing of when echo information is received with the next vocalization, pinna movement, and head movement, especially during close-range targeting [17].

2.2 Head-Movement and Vocalization by Microstimulation

In 2002, Valentine, Sinha, and Moss showed that microstimulation to cells in the SC can produce orienting and vocalizing behaviors in the bat [18]. Through a number of experimental procedures, it was shown that the SC is involved in the pathway of controlling vocal signals and head-movements. The types of responses elicited have similar sweep patterns to a bat in free flight as well.

A second important finding showed that stronger input current stimulations reduced the latency of head movements and vocalizations. Figure 3 below is an illustration from their study showing data points of decreasing latency. Figure 3A specifically shows an important behavior: at any current level, the head movement

always has a lower latency than the vocalization, suggesting that there is a mechanism in place that prevents a vocalization from occurring before the head movement repositions the head for a future vocalization.

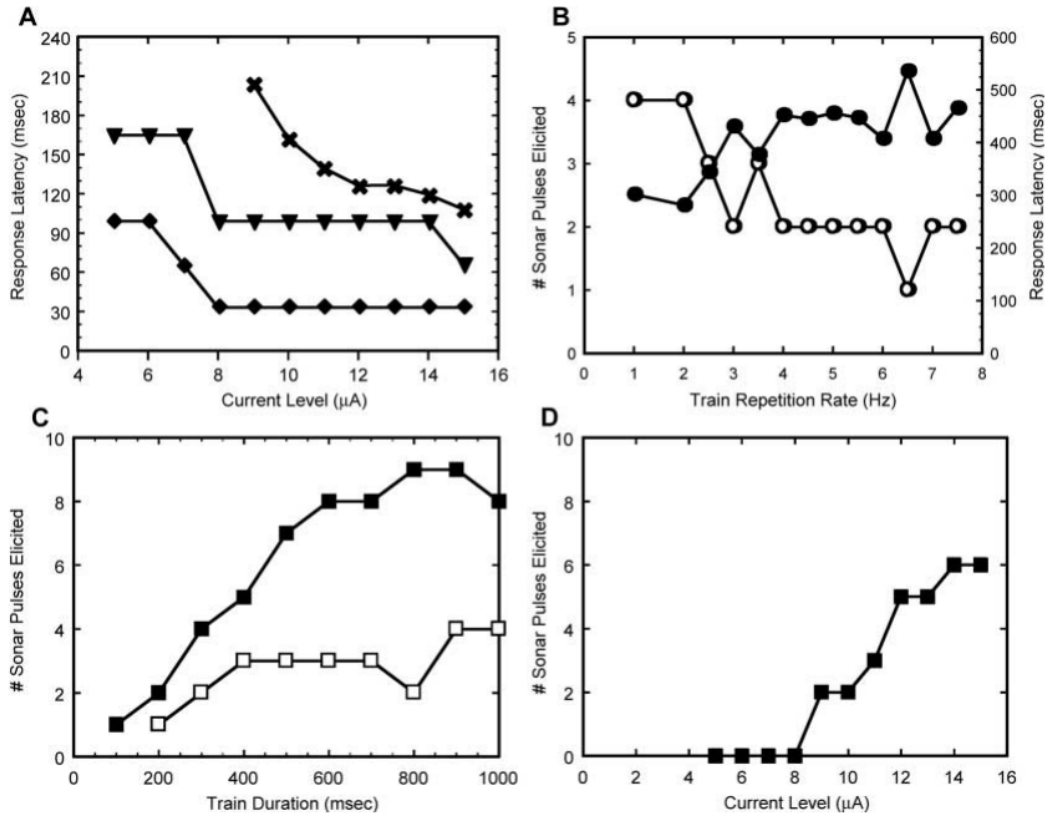


Figure 3. Microstimulation response profiles from Valentine, Sinha, and Moss, 2002 [18]. A) shows the decrease in latency of vocalizations (crosses), head movements (triangles), and pinna movements (diamonds). B) shows the number of sonar pulses (open circles) and the delay (filled circles). C) shows how many vocalizations are emitted for a current level of 10 microamps (open squares) and 13 microamps. D) shows how many pulses are emitted for a pulse train of 200 msec. [18]

While the responses elicited through this microstimulation are consistent with other studies, the properties of the head and pinna movements depend on where the electrode actually stimulates in the SC (what layer, what location on the layer, etc.).

There is some chance that at high current levels, the stimulation may have bled into the periaqueductal gray (PAG), and those neurons may have been partially responsible for the vocalizations. However, this possibility is not consistent with standard current spread from a probe, and chemical injections used earlier in the study isolated that as a concern (control saline injections in the same area did not elicit responses, which would have likely been seen if the PAG was causing the activity).

2.3 Vocal Premotor Activity

In 2007, Sinha and Moss [19] explored the vocal premotor activity in the SC, and showed that there is consistent neural activity before the production of sonar vocalizations and not communication calls, and that the timing between this activity and the call has a direct relationship. Two relationships are most important to the development of the computational model, shown in Figure 4 below. First is the relationship between a call's duration, and the interval between pulses. From a physical standpoint, a longer duration of call would generally contain more power, and be directed towards targets further away. In that sense, a longer pulse interval would be required, so as to give the information enough time to travel back from the object. While there is some variability to this graph there is a defined floor on call duration and pulse interval – that is, as the pulse interval increases, duration will not fall below the 'line' of trials that are at the bottom of the group. This could be the physical limit of how long a call takes to emit and echo back to the bat, be processed, and reoriented to the next call.

The second part of the figure shows the neural activity lead time in relation to how long a call lasts. Shorter calls have shorter lead times. This phenomenon could be a result of a neural integrator circuit being present as part of the SC. Because longer call duration would require more power, the start of neural activity in the SC indicates that some process should start integrating more neurons into activity. Once the actual call needs to be made, this built-up activity discharges and contributes to the call's intensity and duration.

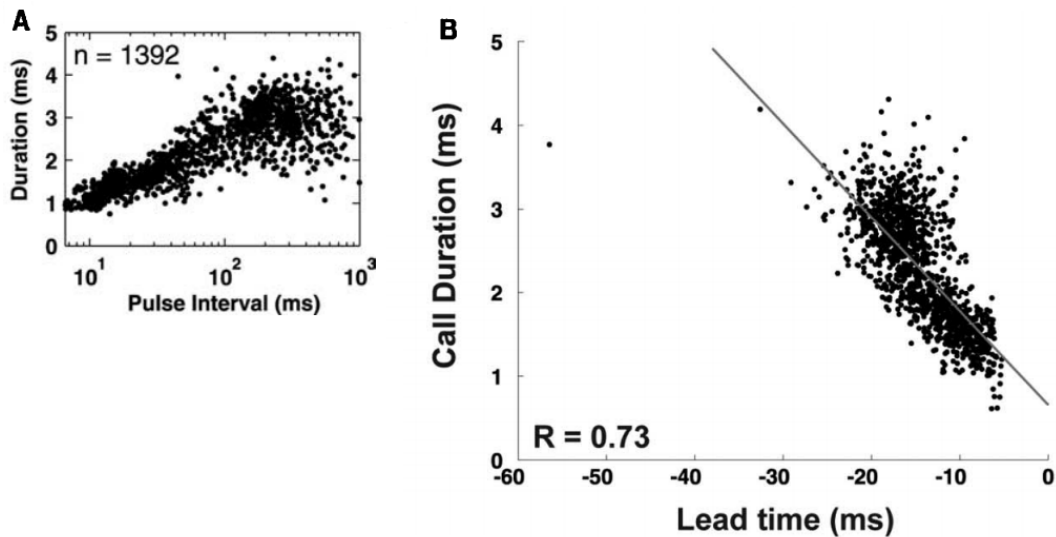


Figure 4. A) Shows the sonar call duration versus pulse interval for all 1392 trial calls on a semilog plot. B) Shows a linear regression of call duration versus activity lead time as an isolated predictor [19].

In accordance with the results of this paper, the change of call length with target distance is parallel to the primate and feline control of depth – they use vergence eye movement pathways, which are suggested to occur in the rostral pole of the SC [20, 21, 22], as well as in cats [23].

Microstimulation of the various areas in the SC area suggest that it participates in the vocal motor control circuit: areas of the auditory cortex and SGN (supragenulate nucleus) project through the frontal cortex, and to the SC in a potential gating context, preventing the SC from sending motor commands until it receives the appropriate ‘go’ signal [24].

Chapter 3: Existing Computational Models of the Superior Colliculus

3.1 Trappenberg et al. (2001)

The model developed by Trappenberg et al. in 2001 [25] is one of the first that integrates exogenous and endogenous signals to initiate saccades through a superior colliculus structure. Behavior of the model follows biological data from the intermediate layers of the SC in monkeys. Effectively, the information received from the inputs is integrated through dynamic competition, with local collicular connections.

The local connections of the SC are modeled to have a “Mexican-hat” shape structure; a unit has excitatory connections to its neighbors, and inhibitory connections – or very weak connections – to cells that are further away.

The model consists of three neuron types: *buildup*, *burst*, and *fixation* neurons (fixation neurons being on the rostral pole of the SC map). Figure 5, adapted from Trappenberg et al., shows the three components and how they fire in a standard task. First, the buildup cells (blue) begin to fire more rapidly, suppressing fixation cells (green). Once activity has built up to a certain level, the saccadic burst neurons (red) generate a quick spike of activity, at which point the cell resets to the pre-saccade state.

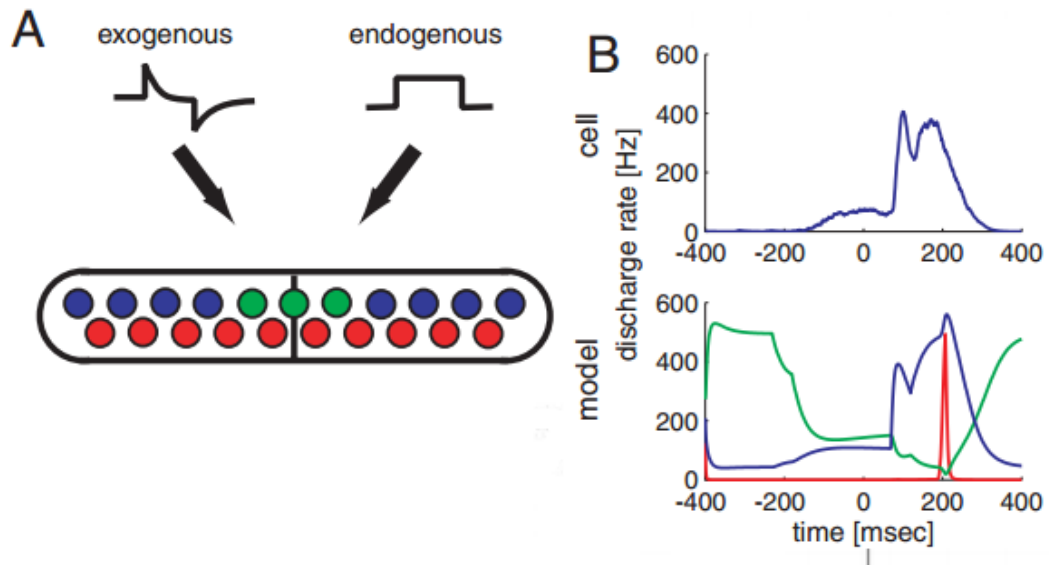


Figure 5. A) Shows the overview of their model. The two types of inputs both affect the buildup neurons (blue). The other neurons react from the buildup's activity, with fixation cells being green, and burst cells being red. B) Shows a sample saccade task. Buildup neurons suppress fixation firing, and activate the burst neurons once reaching a threshold of activity. From Trappenberg et al., 2001. [25]

Their model is one-dimensional, but can be generalized to two dimensions [26]. The model equations implement standard integrate-and-fire neurons, with a noise component that models synaptic connection. The exogenous and endogenous inputs are both simple Gaussian spatial inputs, representing the SNR in lieu of a separate layer of neurons projecting inhibition on the SC.

The interactions within the SC, as mentioned previously, have short-distance excitatory and long-distance inhibitory connections laterally within their layer of the SC.

3.2 Arai and Keller (2005)

In 2005, Arai and Keller [27] developed a two-dimensional saccade model for the visual system. Figure 6 shows the hierarchical view of the system. In this model, the SC drives horizontal and vertical motor groups that negatively feed back to the SC as motion happens. The rest of the model is quite similar to Trappenberg's – this one adds a component for driving motor outputs for the eyes, which, while interesting, doesn't explicitly occur in the SC.

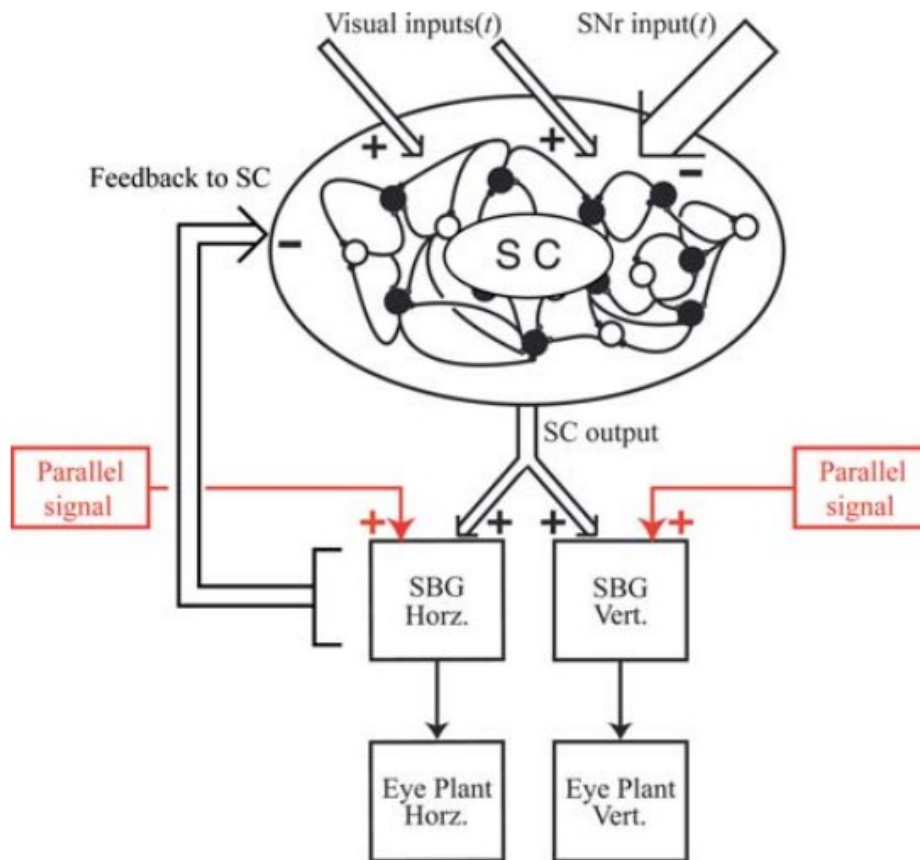


Figure 6. System model for an SC generating saccades. Visual inputs and SNr inputs interact with the SC, which has internal excitatory and inhibitory connections. The outputs from the SC are sent to horizontal and vertical eye movement controllers (SBGs from the brainstem), which feed back to the SC and drive the eye motors. From Arai and Keller, 2005 [27].

3.3 Proposed Non-Spiking Model

The models discussed above, along with the influence of neurophysiological and behavioral data have influenced the current model that is being developed, seen in Figure 7. The core components modeled here are the suppressing SNr layer, the

two SC layers (buildup and burst), the H (horizontal) and V (vertical) burst generators, and their associated interactions with the vocalization-related priming and burst neurons. The function is similar to saccade models discussed earlier, except that the motor vectors associated with different positions describe head movement rather than eye movements.

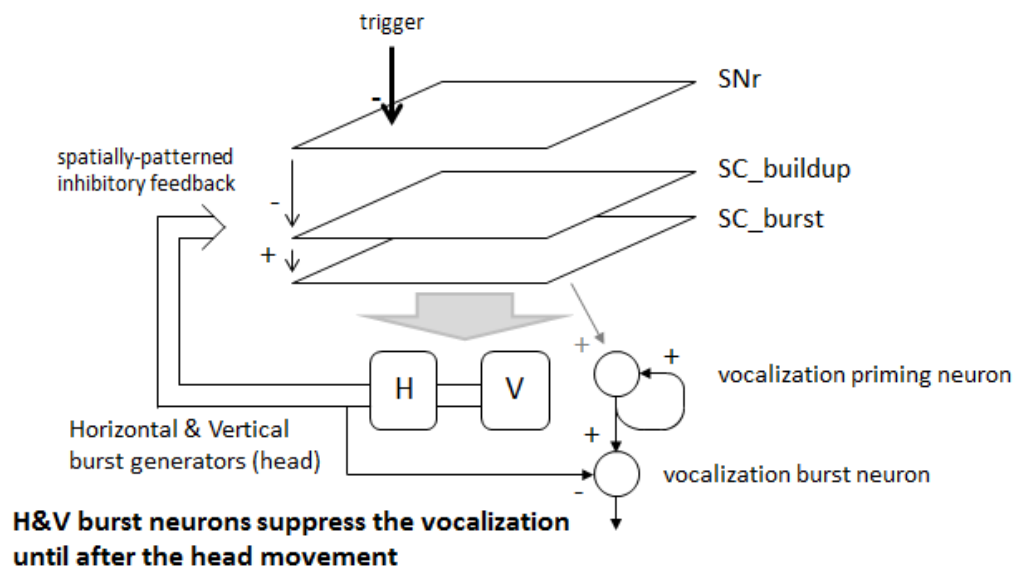


Figure 7. In this model, a 2D SNr field suppresses the natural buildup of activity in the SC buildup layer. If the SNr inhibition is released, the SC will build activity, then cause the burst neurons to drive the horizontal and vertical head-movement motors, which feed back to the SC buildup and burst layers, restoring the previous state. The vocalization priming neuron is triggered by a certain level of activity in the SC, where a signal will build up until it is allowed to discharge through the vocalization burst neuron.

In the mean-rate, or non-spiking model, the SNr inhibition and dis-inhibition is modeled by a continuous variable representing the mean firing rate of a population

of spiking neurons. Normally, the inhibition projected by the SNr strongly suppresses the layers beneath it, preventing buildup activity and thus burst activity. As with Arai and Keller's model, a Gaussian input inhibits the SNr, which allows the SC buildup to begin. The end result of each can be seen in Figure 8.

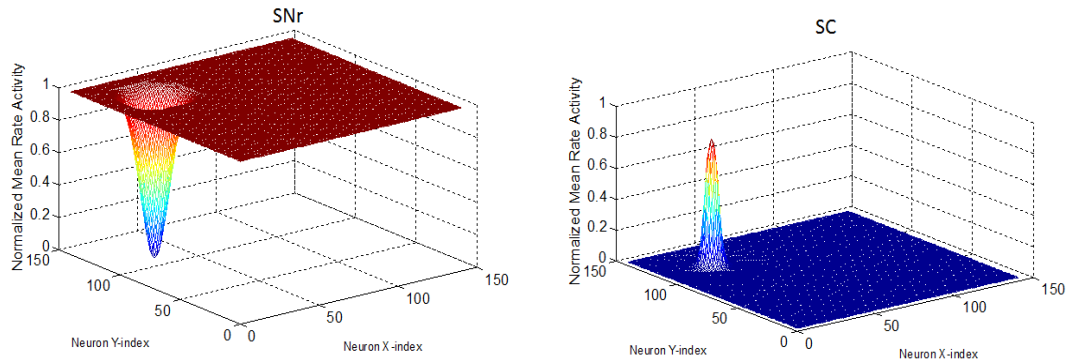


Figure 8. SNr and SC activity some time after a dis-inhibition of an SNr area. The laterally connected SC area directly connected to the SNr has a peak of buildup activity.

The above plots are activity levels after the SC has built up – that is, some time has elapsed (100-150 ms) following the disinhibition while the SC neurons fired and recurrently excite each other. Once this SC buildup has reached a threshold level, the burst neuron is triggered. This can be seen in Figure 9. Once the burst is triggered, the SNr is returned back to its pre-movement state (fully firing), and the SC buildup dies from the restored inhibition.

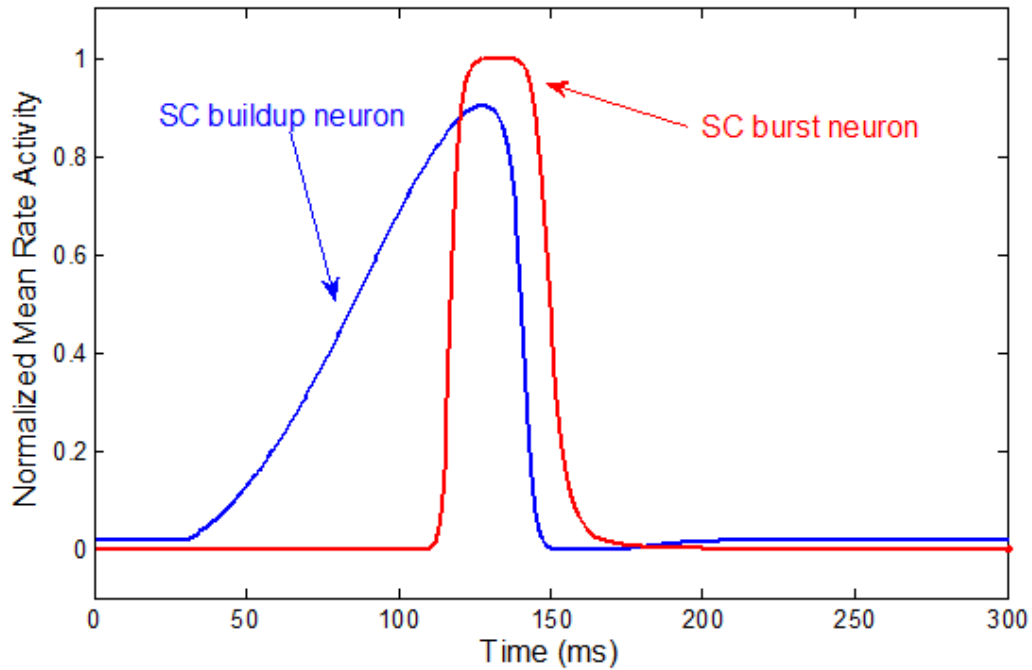


Figure 9. Buildup activity rises to a certain rate of activity, which drives the burst neurons to the horizontal and vertical outputs for head motion. The burst activity feeds back and shuts down the SC buildup and burst firing.

In this version of the model, the mechanisms behind the vocalization and head movement are based on mean-rate variables as well. The SC burst neurons trigger synchronized vertical and horizontal head motion. While the head motion occurs, vocalization is suppressed. Once motion stops, the vocalization can occur. In Figure 10, the resulting vertical and horizontal motions (from the activity vector in Figure 8) are shown. The motor commands (black and blue lines) begin when the burst neurons do, and shut down as the burst stops again. Once the motor signals fall to rest, the vocalization burst neuron fires.

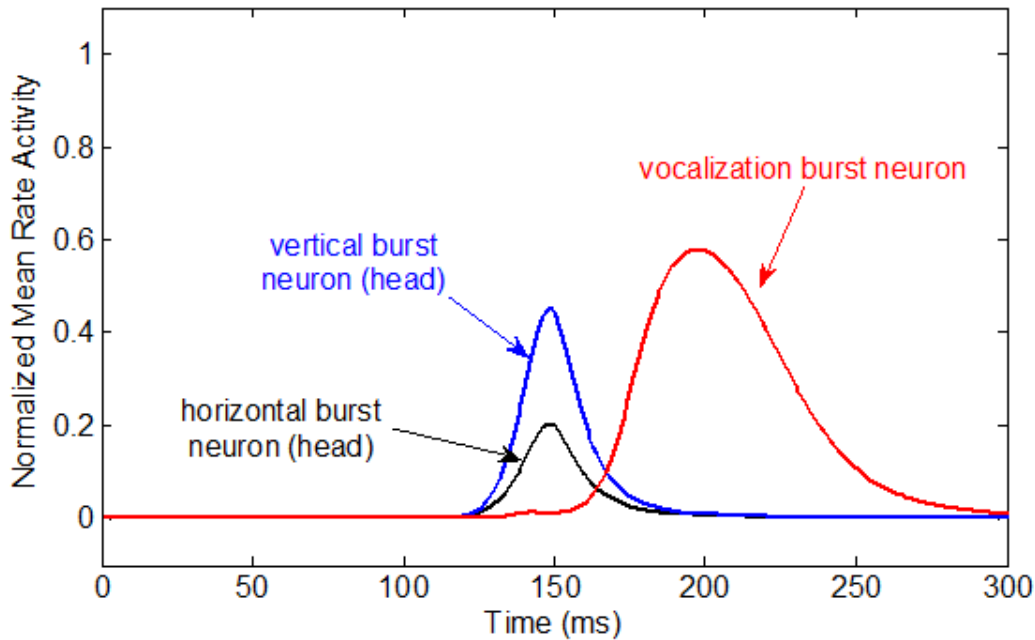


Figure 10. The burst neurons activate the vertical and horizontal motion, as well as the vocalization priming neuron in the background. Head motion suppresses vocalization - once the motion is complete, the vocalization burst begins.

This model differs from the others in that it suggests that there is a mechanism in the SC that coordinates vocalization timing. Previous models have emphasized the eye / saccadic system, of non-bat species where vocalizations are not integral to the sensing process. Beyond simple coordination, however, the SC is likely to actively participate in defining the vocalization magnitude/duration due to its sensitivity to object range and other pre-vocalization signals that have been found that correlate with duration (Sinha and Moss, discussed in Chapter 2.)

The model of the bat superior colliculus is novel in this sense. It is, however, desirable to develop the model further and translate parts of this model into a spiking domain, instead of using only mean-rate firing variables. The next chapter discusses

a spiking neuron version of the SNr, the SC, and the neural integration (which motivates the change in vocalization behavior relative to head-movement in the spike-based model).

Chapter 4: A Spike-Based Model of the Bat Superior Colliculus

The core components of the spiking model are the SC buildup layer, the SNr inhibition layer, and the neural integrator that builds up vocal activity between the start and end of the head motion. The mean-rate neural model of the motor system is incorporated, but not yet in a spiking manner, as they are not components directly in the SC, and the basic results of this part of the model remains the same. The vocalization component, however, in this spiking model is unique. The neural integrator component controls the duration and amplitude of the vocalization. Motivated by the long-lead latency burst seen by Sinha and Moss [19], the magnitude of the vocalization is controlled by the relative timing of two separate signals. The starting trigger of vocalization occurs when the integrator start neuron activates. There is a separate post-integration trigger that allows the vocalization to occur. Once the integrator stop neuron activates, the vocalization may occur. The model diagram shown in Figure 11 shows this component. The vocalization burst neuron will discharge the neural integrator activity.

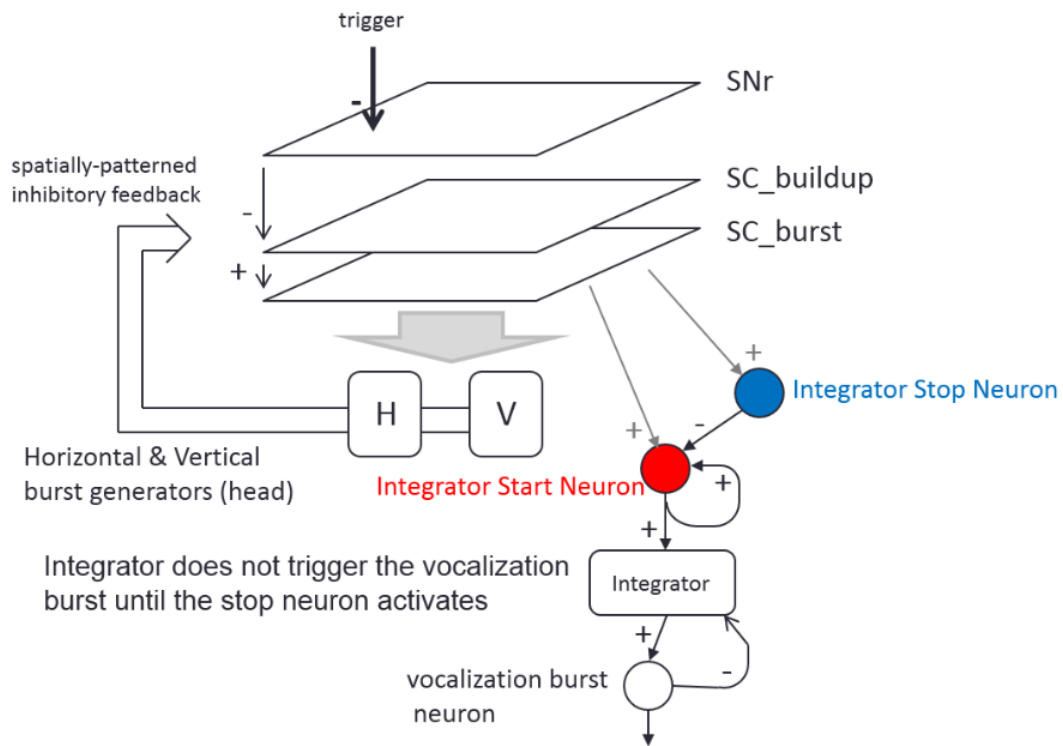


Figure 11. Spiking model of the SC. The main difference between this and the non-spiking model is in the vocalization through a neural integrator. Two signals, the integrator start and stop, control the integrator’s time to start building activity and stop building activity, respectively. The vocalization burst neuron does not become active from the integrator activity until the integrator has completed building up. Once the integrator finishes building, it discharges activity to the burst neuron. SC_burst, horizontal and vertical burst generators, and their feedback are not yet modeled in this spiking version.

4.1 Neuron Model Equations

The SNr neurons in the current model play the role of controlling the inhibition to the SC. This layer is a two-dimensional square array, each controlled by simple integrate-and-fire equations. They are tonically active – that is, in the absence of external input, they will fire at a regular rate.

$$\tau \frac{dV}{dt} = -V + R_m I_{ext}(t)$$

Where τ is the time constant of the neuron, V is the membrane voltage, R_m is the membrane resistance, and I_{ext} is the external current, if any.

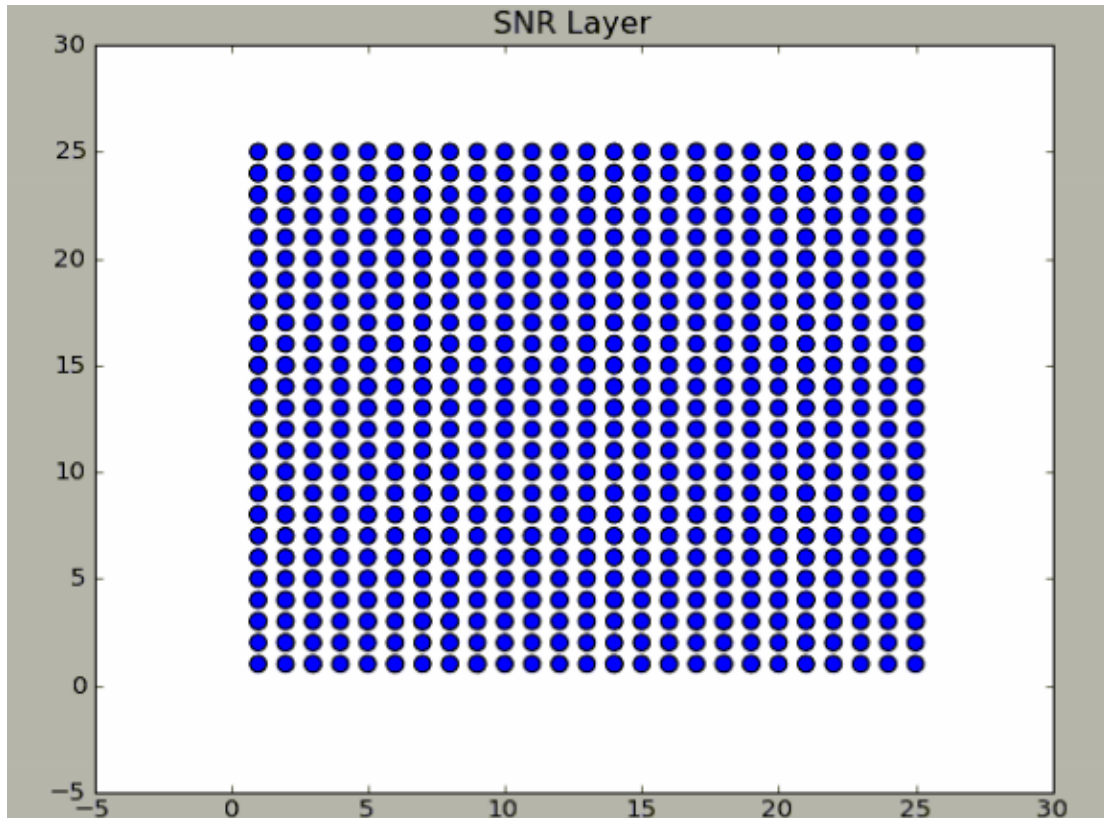


Figure 12. Visual representation of the 2D SNR layer. Each dot represents a neuron, and in this case, the array is 25x25. The SC layers (buildup and burst) have the same layout. The output layer (burst) neurons, representing different 2D head movements, project to the horizontal and vertical head plants with a trigonometric relationship corresponding to the movement direction.

Each neuron in the SNr layer has an inhibitory synapse to the SC buildup layer beneath it, which is also a two-dimensional square of neurons. Both layers are the same size, and they are connected in a one-to-one fashion. The SC layer also uses a similar set of equations. To justify the level of detail in the neuron, it was important to determine what characteristics needed to be captured. The goal of this layer is to recurrently excite neighboring neurons with a Gaussian-shaped projective field, and to produce a ‘hill’ of activity, as seen in Figure 8 (above). The most important feature to correctly model is the 2D recurrent connection matrix. Three levels of neuron complexity were considered for the choice of the SC neuron model: full-scale Hodgkin-Huxley equation representation, Izhikevich-style neurons, and a simple integrate-and-fire with synaptic current as part of the external input. The first, Hodgkin-Huxley, proved too computationally intense to scale to networks of 25x25 neurons and beyond, using excessive time and memory. The complex differential equations did not provide more information than simpler models, and the Izhikevich model produced the same results, with fewer calculations. In the end, however, the same spiking behavior was realized with a simple integrate-and-fire model. Because the primary mode of operation of the model is using mean-rate activity, the detailed spike timing becomes less important –implementing the simplest model that can produce the behavior seen in Figure 8 is desirable, which the integrate-and-fire model does adequately. The same equation used for SNr on page 19 holds for this layer of neurons, but the time constant and membrane resistance were altered to provide different firing rates.

In contrast, the neural integrator requires a more in-depth model to produce the desired integrate-and-hold behavior. The neural integrator must accept a triggered input from the SC, signaling the onset of activity build. The timing of this signal relative to the vocalization is important, as it determines how long and loud the vocalization must be. Once the SC onset is triggered, neurons begin to build up activity through excitatory network pulses. The output of the neural integrator lies in the total activity of the network – the longer the network has to integrate, the more activity is sent to the vocalization premotor neurons. The buildup of activity in this integrator continues until the vocalization burst neuron shuts off the buildup, and prepares the network for discharge. Once both the vocalization burst neuron trigger and vertical and horizontal burst neurons are non-active, the neural integrator begins to discharge activity through inhibitory pulses that are feedback from the vocalization burst neuron. The inspiration for the basic setup comes from a paper by Koulakov and colleagues [28]. Neural integrators have been successfully modeled in the past, with the caveat that they required extremely precise tuning –synaptic strengths needed to be within 1% of working values [36]. The basic structure of a unit in the recurrent network is shown in Figure 13. Each neuron in a unit connects to the other units in the group, and provides excitatory connections to neighboring units in a 1D line. Based on the weights and equations that define these neurons and synapses, input pulses can start a unit into recurrent activity, and a negative current pulse can shut a unit off.

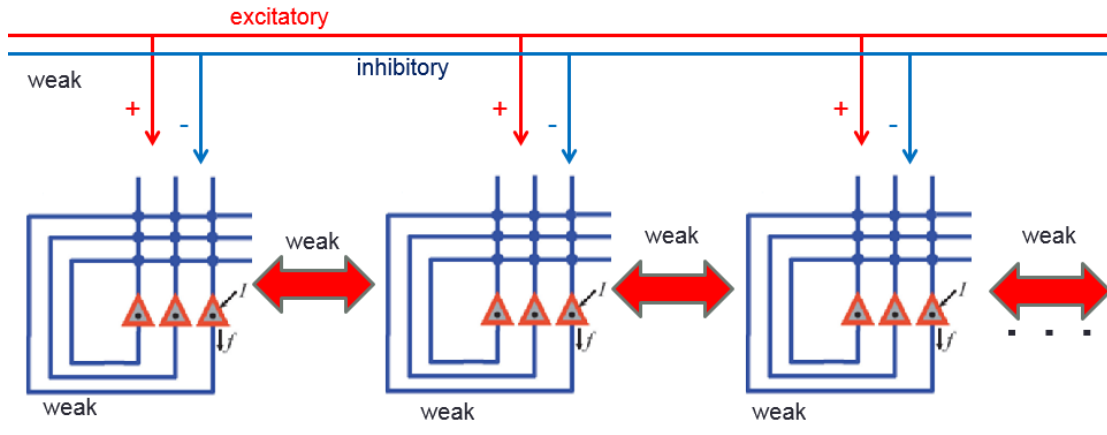


Figure 13. Network connections for the integrator. There are three neurons in each group (the red triangles), with recurrent excitatory connections within the group. Each group also has excitatory connections to other groups in the network, which have the same structure. A global excitatory and inhibitory input (red and blue, respectively) also connects to all groups. These connections are all weak, such that any single input is not sufficient to turn a group on, but inputs from a few, or rapid inputs, may be enough to turn them on. Adapted from Koulakov et al., 2002 [28].

A neural integrator using the same structure but with Izhikevich [29] resonator neurons was built, using a decaying synaptic current connection as described in Figure 13. The result is shown in Figure 14. From left to right, the top three plots are the membrane voltages of each unit. The bottom three plots show the membrane current present in each cell. The equations that describe each neuron are as follows:

$$\frac{dV_m}{dt} = 0.04 * V_m^2 + 5 * V_m + 140 - w + I + I_{feedback} + I_{flat}$$

$$\frac{dw}{dt} = a * (b * V_m - w)$$

$$\frac{dI}{dt} = -\frac{I}{20}$$

$$\frac{dI_{feedback}}{dt} = -\frac{I_{feedback}}{30}$$

The first two equations are characteristic Izhikevich equations, where a , b , and w are constants, and V_m is the membrane voltage $I_{feedback}$ is the recurrent feedback current, I_{flat} is tonic excitation provided to all neurons in the system, and I is the excitation provided by excitatory/inhibitory pulses and current from other units.

At 50 ms, an excitatory pulse generated externally drives the first group to start spiking. The second group doesn't get enough activity to start firing, since it doesn't have support from its neighbor. When another excitatory pulse comes at 250 ms, the second group begins spiking. Group three still does not reach threshold. When an inhibitory pulse occurs at around 600 ms, the second group is shut off, since it does not have excitatory support from group three. Group one does not shut off because it has support from group two and the group that is not shown (background, starter of the chain). Another inhibitory pulse finally shuts off group one.

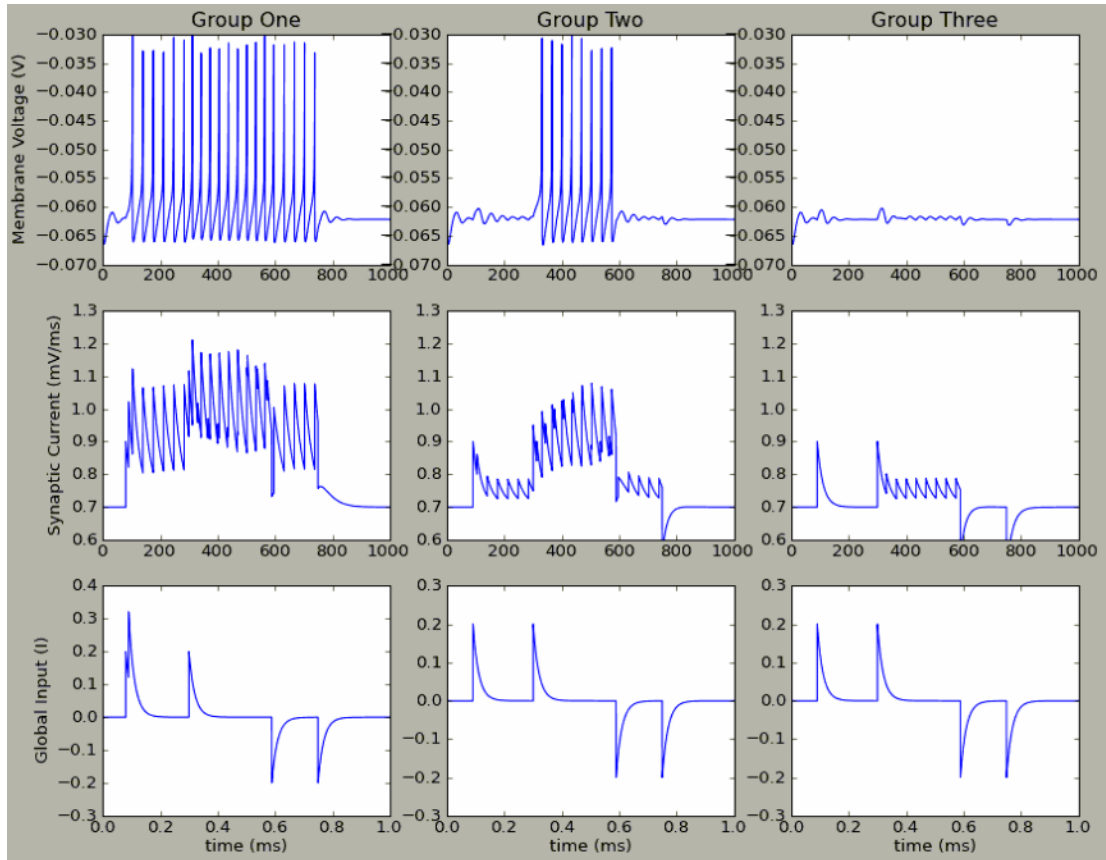


Figure 14. Membrane potentials from a three neuron example of the proposed neural integrator. Neuron #1 is connected to neuron #2, #2 is connected to both #1 and #3 and #3 is connected to #2. Neuron #1 also has an additional excitatory input not shown, to “seed” the integrator. The top row shows the membrane voltage of each cell, the middle row shows the total current that are injected into each neuron, and the bottom row shows the global input with excitatory and inhibitory pulses, intended to turn on and turn off the groups. “At 50 ms, an excitatory pulse to the system latches on neuron #1. At 250 ms, a second excitatory pulse activates neuron #2. Later, two inhibitory pulses at 600ms and 750ms sequentially turn the neurons off. This creates a staircase-like network. A raster of a larger staircase is shown in Figure 13.

The process used to connect these three groups is easily extended to as many groups as necessary. Figure 15 below shows an eight-component neural integrator, with five steps up and four steps down. All code used in this work is included in the appendix.

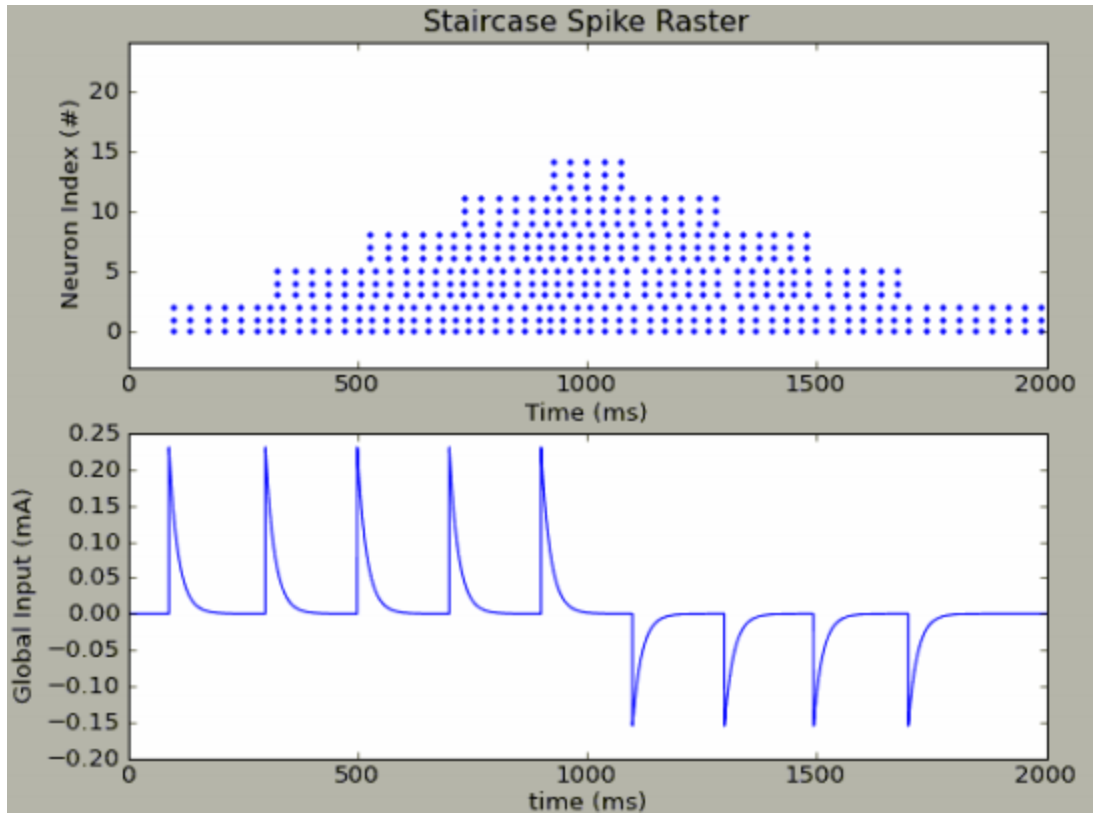


Figure 15. Larger network spike raster. Each group of 3 neurons starts spiking on each excitatory pulse, and one shuts down on an inhibitory pulse. There are five steps up, and then 4 steps down, denoted by the blue arrows. Each step up and step down was separated by approximately 200 ms.

4.2 Connecting the Components

To see how well the model works, it was compared to the non-spiking model discussed at the end of Chapter 3. After configuring the SNr layer neurons to spike at 50 Hz, it suppresses the firing of a small group centered at neuron index (9,9) in the SC. Figure 16 shows the resulting firing rate after being inhibited. Following this disinhibition, the SC layer should have a similar (but inverted) pattern of activity in the same location. The firing rate increases dramatically compared to the low base firing rate of the rest of the neurons, as seen in Figure 16 in the right panel.

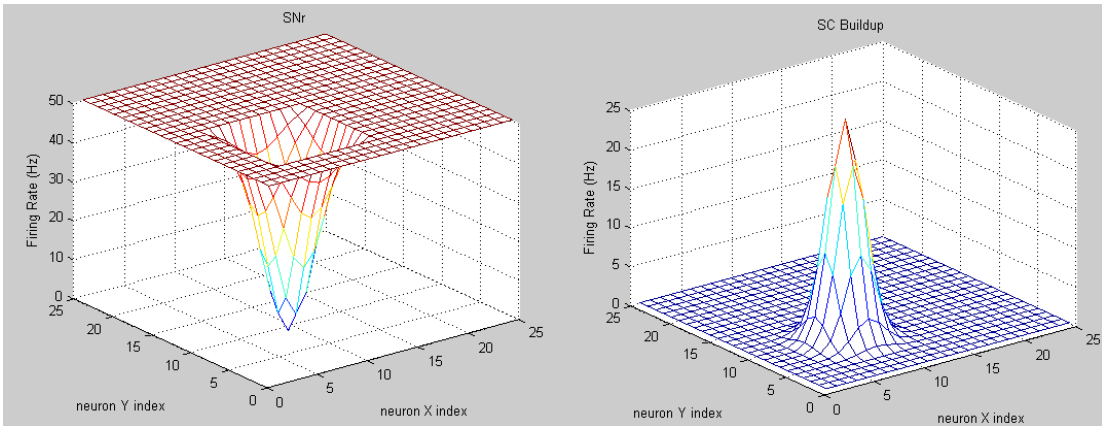


Figure 16. Firing rate results of the spiking model for the SNr and SC buildup neurons. These figures are analogous to those in figure 8. In this simulation, the layer of cells is only 25x25 rather than 150 by 150.

This illustration shows that the connectivity between layers is functioning properly. At locations where the SNr is strongly firing spikes, the SC is completely shut down and does not even reach spiking threshold, whereas at locations where the SNr is suppressed, the SC neurons reach a firing rate of almost 25 Hz.

Once the SC buildup reaches a rate over 20 Hz, the same cascade of events that drive a head movement and vocalization as described in Figure 7 begins. Here, the vocalization integration trigger starts the neural integrator, which determines the magnitude and length of the vocalization (analogous to the red line in Figure 10). Using the SC spikes, and translating it to a mean rate activity output, using the non-spiking model's horizontal and burst.

When the integration start neuron activates, the neural integrator starts to build activity, in the staircase fashion seen above in Figure 15. The integrator stop neuron will stop the neural integration, and will start the discharge of the integrator into the

vocalization burst neuron. The activity strength in the neural integrator at the start of discharge determines the strength and length of the call. The longer the neural integrator has to build activity, both the longer and louder the vocalization will be. The output of the neural integrator is the amount of activity that was built up.

The signal start and stop neurons are not locally defined at a specific area of the SC yet. To this point, there exists no direct biological data that would pinpoint these signals in a specific area. One hypothesis is that the signals are embedded in the pause neurons in the rostral pole.

The spiking model for the SNr, SC, and neural integrator parts of this model successfully implement the desired behavior of this system. Relatively simple neurons work together to create spiking network behavior that has been seen in biological experiments.

4.3 VLSI Considerations

The SNr and SC integrate-and-fire model networks have been implemented numerous times in silicon [30, 31, 32, 33]. Some possible characteristics that could be implemented to make the model more biophysical, such as probabilistic synapses and synaptic plasticity, also have some versions of silicon fabrication [34].

Since the neural integrator is modeled as a network of Izhikevich neurons, it would necessitate different VLSI units [35]. The chip developed by Rangan and Sundeep [35] models simple Izhikevich units, but the basic structure could be repeated and combined with the previously discussed VLSI synapses to allow for

plasticity in synaptic strengths and probabilistic synapses. VLSI circuits will also not have an issue simulating large neuron arrays. The units are small enough that realistically sized networks can be implemented.

Chapter 5: Future Work

Although this model of the bat superior colliculus is still in its infancy, it provides a foundation for defining and incorporating the role it plays in echolocation behavior. Further development of the model could be biophysical, incorporating larger neuron groups and probabilistic synapses with noise, and additional spiking components, such as the horizontal and vertical burst neurons that drive the head movement.

First, almost all biological systems need to adapt to sources of noise, whether they come from motor, sensory, or internal (e.g., neural) sources. It would be beneficial to develop a model for different noise sources and inject them appropriately into the network.

Currently, the neuron groups in the simulated model consist of single neurons or small neuron groups. In the biological system, the neurons are probably functionally members of overlapping groups. Instead, individual nodes could be multi-neuron units with connections that are perhaps dense or sparse, depending on the size.

Appendix A: Python Code (BRIAN script for defining the network)

```
"""
Last Modified on Apr 24, 2013

@author: Matt
"""
from brian import *
import csv
import math
#Neuron model parameters
Vr_SCBuildup = -65*mV
Vt_SCBuildup = -55*mV
El_SCBuildup = -50 * mvolt

Vr_SNR = -70*mV
Vt_SNR = -55*mV
El_SNR = -30*mV #Natural spiking

Vr_input = -70*mV
Vt_input = -55*mV
El_input = -30*mV #Natural Spiking

Vr_test = -65*mV
Vt_test = -55*mV
El_test = -30*mV

tau = 10 * msecond

weight = 1.86 * mV

square=25

SCBuildup_Eqs = Equations("""
    dV/dt = -( V - El_SCBuildup)/(3.3*tau) + If*25 : volt
    dIf/dt = -If/(.3*tau) : mvolt/ms
""")
```

```

test_Eqs = Equations("""
    dV/dt = -(V-El_test)/(.1*tau) : volt
    """)
SNR_Eqs = Equations("""
    dV/dt = -(V-El_SNR)/(1.4*tau) : volt
    """)

SNR = NeuronGroup(N=square*square, model=SNR_Eqs,
threshold=Vt_SNR,reset=Vr_SNR,refractory=1*ms)

SCBuildup = NeuronGroup(N=square*square, model=SCBuildup_Eqs,
threshold=Vt_SCBuildup,reset=Vr_SCBuildup,refractory=1*ms)

test_input = NeuronGroup(N=1, model=test_Eqs,
threshold=Vt_test,reset=Vr_test,refractory=1*ms)

SCBuildup_sub = [SCBuildup.subgroup(1) for i in range(square*square)]
SNR_sub = [SNR.subgroup(1) for i in range(square*square)]

C_SCBuildup = Connection(SCBuildup,SCBuildup,'If')

C_SNR_SC = Connection(SNR,SCBuildup,'If')

C_SNR_SC.connect_one_to_one(SNR,SCBuildup,-weight*15)

#all connections
for i in range(1,square*square):
    index = i-1
    row = math.floor(index/square)
    column = index%(square)
    for j in range(1,square*square):
        if(j!=i):
            row2 = math.floor((j-1)/square)
            column2 = (j-1)%(square)
            weight2=15*weight*math.exp(-math.sqrt((row2-row)*(row2-row)+(column2-
column)*(column2-column)))
            C_SCBuildup.connect(SCBuildup_sub[index],SCBuildup_sub[j-1],weight2)

C_test = Connection(test_input,SNR,'V');
#Center cross

```

```

C_test.connect(test_input,SNR_sub[square*square/2],-weight*4)
C_test.connect(test_input,SNR_sub[square*square/2-1],-weight*1.3)
C_test.connect(test_input,SNR_sub[square*square/2+1],-weight*1.3)
C_test.connect(test_input,SNR_sub[square*square/2+square],-weight*1.3)
C_test.connect(test_input,SNR_sub[square*square/2-square],-weight*1.3)
#Center diagonals
C_test.connect(test_input,SNR_sub[square*square/2+square+1],-weight*1.1)
C_test.connect(test_input,SNR_sub[square*square/2-square+1],-weight*1.1)
C_test.connect(test_input,SNR_sub[square*square/2+square-1],-weight*1.1)
C_test.connect(test_input,SNR_sub[square*square/2-square-1],-weight*1.1)
#Added cross
C_test.connect(test_input,SNR_sub[square*square/2+square+square],-weight*1.1)
C_test.connect(test_input,SNR_sub[square*square/2-square-square],-weight*1.1)
C_test.connect(test_input,SNR_sub[square*square/2+2],-weight*1.1)
C_test.connect(test_input,SNR_sub[square*square/2-2],-weight*1.1)

#For the scatterplot display
x = []
y = []
y1 = []
for i in range(1,square+1):
    x1 = [i]
    x2 = []
    y2 = [i]
    for i in range(1,square+1):
        x2.extend(x1)
    x.extend(x2)
    y1.extend(y2)

for i in range(1,square+1):
    y.extend(y1)

SCBuildup.V = Vr_SCBuildup + rand(len(SCBuildup)) * (Vt_SCBuildup-
Vr_SCBuildup)
SNR.V = Vr_SNR + rand(len(SNR)) * (Vt_SNR-Vr_SNR)

counter_SNR = SpikeCounter(SNR)
spike_SNR = SpikeMonitor(SNR)
counter_SCBuildup = SpikeCounter(SCBuildup)
spike_SCBuildup = SpikeMonitor(SCBuildup)

```

```

state_test = StateMonitor(test_input,'V',record=True)
state_SCBuildup = StateMonitor(SCBuildup,'V',record=True)

run(300*ms, report='stderr')

center = square*square/2

figure(1)
subplot(211)
title("SNR Layer")
scatter(x,y,s=5*counter_SNR.count)
subplot(212)
title("SC Layer")
scatter(x,y,s=5*counter_SCBuildup.count)
figure(2)
subplot(211)
title("SNR Raster")
raster_plot(spike_SNR)
subplot(212)
title("SC Buildup Raster")
raster_plot(spike_SCBuildup)
figure(3)
subplot(311)
plot(state_SCBuildup.times,state_SCBuildup[312])
subplot(312)
plot(state_SCBuildup.times,state_SCBuildup[312+1])
subplot(313)
plot(state_SCBuildup.times,state_SCBuildup[312+square+2])

show()

# Neural Integrator Code
'''
Updated April 10, 2013

@author: Matt
'''
from brian import *
from brian.library.IF import *
import time

```

```

a=0.1/ms
b=0.25/ms

num = 3;

eqs = Equations("""
    dvm/dt=(0.04/ms/mV)*vm**2+(5/ms)*vm+140*mV/ms-w+I+Ifeedback+Iflat
: volt
    dw/dt=a*(b*vm-w) : volt/second
    dI/dt=-I/20/ms : volt/second
    dIfeedback/dt = -Ifeedback/30/ms : volt/second
    Iflat : volt/second
    Itotal = Ifeedback + I + Iflat:volt/second
""")

eqsRS = Izhikevich(a=0.1/ms,b=0.26/ms)
resetRS = AdaptiveReset(Vr=-65*mV,b=2.0*nA)

group = NeuronGroup(N=num,model=eqs,threshold=-30*mV,reset=resetRS)
group2 = NeuronGroup(N=num,model=eqs,threshold=-30*mV,reset=resetRS)
group3 = NeuronGroup(N=num,model=eqs,threshold=-30*mV,reset=resetRS)

#Pinput = PulsePacket(t=90*ms,n=1,sigma=0*ms)
spiketimes = [(0,90*ms), (0,300*ms)]
spiketimes2 = [(0,589*ms), (0,750*ms)]
Pinput = SpikeGeneratorGroup(1,spiketimes);

#Pinput2 = PulsePacket(t=589*ms,n=1,sigma=0*ms)
Pinput2 = SpikeGeneratorGroup(1,spiketimes2);

PinitialInput = PulsePacket(t=80*ms,n=1,sigma=0*ms)

#Connect input *full* to everything
C = Connection(Pinput,group,'I');
C2 = Connection(Pinput,group2,'I');
C3 = Connection(Pinput,group3,'I');

Cinitial = Connection(PinitialInput,group,'I');
Cin2to1 = Connection(Pinput2,group,'I');
Cin2to2 = Connection(Pinput2,group2,'I');
Cin2to3 = Connection(Pinput2,group3,'I');
Cfeedback = Connection(group,group,'Ifeedback');

```

```

Cfeedback2 = Connection(group2,group2,'Ifeedback');

C1to2 = Connection(group,group2,'Ifeedback');
C2to1 = Connection(group2,group,'Ifeedback');
C2to3 = Connection(group2,group3,'Ifeedback');

C.connect_full(weight=0.2*mV/ms);
C2.connect_full(weight=0.2*mV/ms);
C3.connect_full(weight=0.2*mV/ms);

Cinitial.connect_full(weight=0.2*mV/ms);
Cin2to1.connect_full(weight=-0.2*mV/ms);
Cin2to2.connect_full(weight=-0.2*mV/ms);
Cin2to3.connect_full(weight=-0.2*mV/ms);

Cfeedback.connect_full(weight=(0.2/num + 0.2/10)*mV/ms);
Cfeedback2.connect_full(weight=0.2/num*mV/ms);
C1to2.connect_full(weight=0.2/10*mV/ms);
C2to1.connect_full(weight=0.2/10*mV/ms);
C2to3.connect_full(weight=0.2/10*mV/ms);

M = StateMonitor(group,'vm',record=True)
N = StateMonitor(group,'Itotal',record=True)
O = [SpikeMonitor(group)]
M2 = StateMonitor(group2,'vm',record=True)
N2 = StateMonitor(group2,'Itotal',record=True)
O2 = [SpikeMonitor(group2)]
M3 = StateMonitor(group3,'vm',record=True)
N3 = StateMonitor(group3,'Itotal',record=True)
O3 = [SpikeMonitor(group3)]

Mpp= [SpikeMonitor(Pinput)]

group.vm=-63*mV
group.w=-14*mV/ms
group.Iflat=.70*mV/ms
group2.vm=-63*mV
group2.w=-14*mV/ms
group2.Iflat=.70*mV/ms
group3.vm=-63*mV
group3.w=-14*mV/ms
group3.Iflat=.70*mV/ms
run(1000*ms)

```

```
figure(1)
subplot(231)
plot(M.times/ms,M[0])
ylabel('Voltage (V)')
title('Unit One')
subplot(234)
plot(N.times/ms,N[0])
ylabel('Voltage (V)')
xlabel('time (ms)')
#subplot(337)
#raster_plot(*O)
subplot(232)
plot(M.times/ms,M2[0])
title('Unit Two')
subplot(235)
plot(N.times/ms,N2[0])
xlabel('time (ms)')
#subplot(338)
#raster_plot(*O2)
subplot(233)
plot(M.times/ms,M3[0])
title('Unit Three')
subplot(236)
plot(N.times/ms,N3[0])
xlabel('time (ms)')
#subplot(339)
#raster_plot(*O3)

#figure(2)
#raster_plot(*Mpp)
show()
```

Bibliography

- [1] Schuller, Gerd, and Susanne Radtke-Schuller. "Neural control of vocalization in bats: mapping of brainstem areas with electrical microstimulation eliciting species-specific echolocation calls in the rufous horseshoe bat." *Experimental brain research* 79.1 (1990): 192-206.
- [2] Griffin, D. R., A. Novick, and M. Kornfield. "The sensitivity of echolocation in the fruit bat, *Rousettus*." *The Biological Bulletin* 115.1 (1958): 107-113.
- [3] Lawrence, Beatrice D., and James A. Simmons. "Measurements of atmospheric attenuation at ultrasonic frequencies and the significance for echolocation by bats." *The Journal of the Acoustical Society of America* 71 (1982): 585.
- [4] Simmons J.A.: The resolution of target range by echolocating bats. *J. acoust. Soc. Amer.* 54. 157-173 (1973).
- [5] Valentine, Doreen E., and Cynthia F. Moss. "Spatially selective auditory responses in the superior colliculus of the echolocating bat." *The Journal of neuroscience* 17.5 (1997): 1720-1733.
- [6] Jen, Philip Hungsun, and Xinde Sun. "Pinna orientation determines the maximal directional sensitivity of bat auditory neurons." *Brain research* 301.1 (1984): 157-161.
- [7] Schnupp, Jan WH, and Andrew J. King. "Coding for auditory space in the nucleus of the brachium of the inferior colliculus in the ferret." *Journal of neurophysiology* 78.5 (1997): 2717-2731.

- [8] King, A. J., and M. E. Hutchings. "Spatial response properties of acoustically responsive neurons in the superior colliculus of the ferret: a map of auditory space." *Journal of neurophysiology* 57.2 (1987): 596-624.
- [9] Middlebrooks, JOHN C., and ERIC I. Knudsen. "A neural code for auditory space in the cat's superior colliculus." *The Journal of neuroscience* 4.10 (1984): 2621-2634.
- [10] Palmer, A. R., and A. J. King. "The representation of auditory space in the mammalian superior colliculus." (1982): 248-249.
- [11] Knudsen, E. I., and M. S. Brainard. "Creating a unified representation of visual and auditory space in the brain." *Annual review of neuroscience* 18.1 (1995): 19-43.
- [12] Stein, Barry E., and M. Alex Meredith. "The merging of the senses." (1993).
- [13] du Lac, S. A. S. C. H. A., and ERIC I. Knudsen. "Neural maps of head movement vector and speed in the optic tectum of the barn owl." *Journal of Neurophysiology* 63.1 (1990): 131-146.
- [14] Masino, Tom, and Eric I. Knudsen. "Horizontal and vertical components of head movement are controlled by distinct neural circuits in the barn owl." (1990): 434-437.
- [15] Ewert J-P (1997): Neural correlates of key stimulus and releasing mechanism: a case study and two concepts. *Trends Neurosci* 20: 332–339.
- [16] Hartline, Peter H., Leonard Kass, and Michael S. Loop. "Merging of modalities in the optic tectum: infrared and visual integration in rattlesnakes." *Science* 199.4334 (1978): 1225-1229.

- [17] Kick, SHELLEY A., and JAMES A. Simmons. "Automatic gain control in the bat's sonar receiver and the neuroethology of echolocation." *The Journal of neuroscience* 4.11 (1984): 2725-2737.
- [18] Valentine, Doreen E., Shiva R. Sinha, and Cynthia F. Moss. "Orienting responses and vocalizations produced by microstimulation in the superior colliculus of the echolocating bat, *Eptesicus fuscus*." *Journal of Comparative Physiology A* 188.2 (2002): 89-108.
- [19] Sinha, Shiva R., and Cynthia F. Moss. "Vocal premotor activity in the superior colliculus." *The Journal of neuroscience* 27.1 (2007): 98-110.
- [20] Optican, L. M., and F. A. Miles. "Visually induced adaptive changes in primate saccadic oculomotor control signals." *Journal of neurophysiology* 54.4 (1985): 940-958.
- [21] Gnadt, James W., and Janine Beyer. "Eye movements in depth: What does the monkey's parietal cortex tell the superior colliculus?." *Neuroreport* 9.2 (1998): 233-237.
- [22] Chaturvedi, Vivek, and Jan AM Van Gisbergen. "Stimulation in the rostral pole of monkey superior colliculus: effects on vergence eye movements." *Experimental brain research* 132.1 (2000): 72-78.
- [23] Suzuki, Shunichi, Yasuo Suzuki, and Kenji Ohtsuka. "Convergence eye movements evoked by microstimulation of the rostral superior colliculus in the cat." *Neuroscience research* 49.1 (2004): 39-45.

- [24] Kobler, James B., Susan F. Isbey, and John H. Casseday. "Auditory pathways to the frontal cortex of the mustache bat, *Pteronotus parnellii*." *Science* 236.4803 (1987): 824-826.
- [25] Trappenberg, Thomas P., et al. "A model of saccade initiation based on the competitive integration of exogenous and endogenous signals in the superior colliculus." *Journal of Cognitive Neuroscience* 13.2 (2001): 256-271.
- [26] Taylor, J. G. (1999). Neural bubble dynamics in two dimensions: I. Foundations. *Biological Cybernetics*, 80, 393–409.
- [27] Arai, Kuniharu, and Edward L. Keller. "A model of the saccade-generating system that accounts for trajectory variations produced by competing visual stimuli." *Biological cybernetics* 92.1 (2005): 21-37.
- [28] Koulakov, Alexei A., et al. "Model for a robust neural integrator." *Nature neuroscience* 5.8 (2002): 775-782.
- [29] Izhikevich, Eugene M. "Simple model of spiking neurons." *Neural Networks, IEEE Transactions on* 14.6 (2003): 1569-1572.
- [30] Chicca, Elisabetta, Giacomo Indiveri, and Rodney J. Douglas. "An event-based VLSI network of integrate-and-fire neurons." *Circuits and Systems, 2004. ISCAS'04. Proceedings of the 2004 International Symposium on*. Vol. 5. IEEE, 2004.
- [31] Bartolozzi, Chiara, and Giacomo Indiveri. "Synaptic dynamics in analog VLSI." *Neural Computation* 19.10 (2007): 2581-2603.

- [32] Liu, Shih-Chii, and Rodney Douglas. "Temporal coding in a silicon network of integrate-and-fire neurons." *Neural Networks, IEEE Transactions on* 15.5 (2004): 1305-1314.
- [33] Fusi, Stefano, and Maurizio Mattia. "Collective behavior of networks with linear (VLSI) integrate-and-fire neurons." *Neural Computation* 11.3 (1999): 633-652.
- [34] Goldberg, David H., Gert Cauwenberghs, and Andreas G. Andreou. "Probabilistic synaptic weighting in a reconfigurable network of VLSI integrate-and-fire neurons." *Neural Networks* 14.6-7 (2001): 781-794.
- [35] Rangan, Sundeep. "Estimation with random linear mixing, belief propagation and compressed sensing." *Information Sciences and Systems (CISS), 2010 44th Annual Conference on*. IEEE, 2010.
- [36] Seung, H. Sebastian, et al. "Stability of the memory of eye position in a recurrent network of conductance-based model neurons." *Neuron* 26.1 (2000): 259-271.